Permeation and Interaction of Monovalent Cations with the cGMP-gated Channel of Cone Photoreceptors

ARTURO PICONES and JUAN I. KORENBROT

From the Department of Physiology, School of Medicine, University of California at San Francisco, San Francisco, California 94143

ABSTRACT We measured the ion selectivity of cGMP-dependent currents in detached membrane patches from the outer segment of cone photoreceptors isolated from the retina of striped bass. In inside-out patches excised from either single or twin cones the amplitude of these currents, under symmetric ionic solutions, changed with the concentration of cGMP with a dependence described by a Hill equation with average values, at +80 mV, of K_m = 42.6 μM and n = 2.49. In the absence of divalent cations, and under symmetric ionic solutions, the *I-V* curves of the currents were linear over the range of −80 to +80 mV. The addition of Ca altered the form of the *I-V* curve to a new function well described by an empirical equation that also describes the *I-V* curve of the photocurrent measured in intact photoreceptors. The monovalent cation permeability sequence of the cGMP-gated channels in the absence of divalent ions was $P_K > P_{Na} = P_{Li} = P_{Rb} > P_{Cs}$ (1.11 > 1.0 = 0.99 = 0.96 > 0.82). The conductance selectivity sequence at +80 mV was $G_{Na} = G_K > G_{Rb} > G_{Cs} > G_{Li}$ (1.0 = 0.99 > 0.88 > 0.74 > 0.60). The organic cations tetramethylammonium (TMA) and arginine partially blocked the current, but the larger ion, arginine, was permeant, whereas the smaller ion, TMA, was not. The amplitude of the outward current through the channels increased with the concentration of monovalent cations on the cytoplasmic membrane surface, up to a saturating value. The increase was well described by the adsorption isotherm of a single ion binding site within the channel with average binding constants, at +80 mV, of 104 mM for Na and 37.6 mM for Li. By assuming that the ion channel contains a single ion binding site in an energy trough separated from each membrane surface by an energy barrier, and using Eyring rate theory, we simulated *I-V* curves that fit the experimental data measured under ionic concentration gradients. From this fit we conclude that the binding site interacts with one ion at a time and that the energy barriers are asymmetrically located within the membrane thickness. Comparison of the quantitative features of ion permeation and interaction between the cGMP-gated channels of rod and cone photoreceptors reveals that the ion binding sites are profoundly different in the two types of channels. This

Address reprint requests to Dr. Juan I. Korenbrot, Dept. of Physiology, School of Medicine, Box 0444, University of California at San Francisco, San Francisco, CA 94143.

J. GEN. PHYSIOL. © The Rockefeller University Press · 0022-1295/92/10/0647/27 $2.00
Volume 100 October 1992 647–673

molecular difference may be particularly important in explaining the differences in the transduction signal of each receptor type.

INTRODUCTION

Transduction of light into changes in membrane current in rod and cone photoreceptors of the vertebrate retina results from the coordinated activation of enzymes that control the cytoplasmic concentration of cyclic GMP (reviewed in Pugh and Cobbs, 1986; McNaughton, 1990; Pugh and Lamb, 1990). Cytoplasmic cGMP controls the opening and closing of specific ion channels located in the plasma membrane of the photoreceptor's outer segment (reviewed in Yau and Baylor, 1989; Kaupp, 1991). The biophysical properties of these cGMP-gated channels differ in their quantitative characteristics in rods and cones. In intact rods, for example, the current–voltage (*I-V*) relationship of the cGMP-regulated, light-sensitive currents exhibits pronounced outward rectification at positive voltages and near voltage independence in the range between −30 and −60 mV (Baylor and Nunn, 1986; Hestrin and Korenbrot, 1987). In cones, on the other hand, the same currents exhibit outward rectification at positive voltages, but they are voltage dependent in the range between −30 and −60 mV (Attwell, Werblin, and Wilson, 1982.[1] Studies in membrane patches excised from either rods or cones have demonstrated that some of the current rectification arises from a voltage-dependent block of open channels by divalent cation (reviewed in Yau and Baylor, 1989). However, even in the absence of divalent ions, cGMP-dependent currents in excised rod membrane patches continue to exhibit outward rectification at positive voltages (Karpen, Zimmerman, Stryer, and Baylor, 1988), whereas those in cone membranes do not (Haynes and Yau, 1985). Indeed, the difference in rectification characteristics between rods and cones is apparent even at the single channel level: the current through single cGMP-gated channels is linear with voltage in cone membranes (Haynes and Yau, 1990), but rectifies in an outward direction in rod membranes (Ildefonse and Bennett, 1991).

The cGMP-gated channels are permeable to monovalent and divalent cations in both rods and cones (reviewed in Yau and Baylor, 1989; Korenbrot and Maricq, 1991). However, recent studies in intact cone photoreceptors have suggested that the permeation of divalent cations may differ in the rod and cone channels (Perry and McNaughton, 1991).[1] The ion selectivity of cGMP-gated channels in rods has been extensively investigated, beginning with the examination of ion selectivity of light-sensitive currents in intact cells (Yau, McNaughton, and Hodgkin, 1981; Yau and Nakatani, 1984; Hodgkin, McNaughton, and Nunn, 1985; Menini, Rispoli, and Torre, 1988) and culminating with studies in detached membrane patches (Furman and Tanaka, 1990; Menini, 1990). In cones, the selectivity of light-sensitive currents in intact cells has only recently been investigated (Perry and McNaughton, 1991), and studies in detached patches have not appeared previously. We report here an analysis of the monovalent cation selectivity of cGMP-gated currents in membrane patches excised from cone outer segment. Indeed, we find important differences in the permeation and interaction of monovalent cations with the cGMP-gated channels in the two receptor types. This variance may provide important functional clues in

[1]Miller, J. L., and J. I. Korenbrot, manuscript submitted for publication.

understanding the differences in the characteristics of the transduction signals in rods and cones.

MATERIALS AND METHODS

Materials

Striped bass (*Morone saxatilis*), obtained from a fish hatchery (Professional Aquaculture Services, Chico, CA), were maintained in the laboratory for up to 4 wk under 12-h dark–light cycles with free access to fish chow. Fish used for experimentation were 7–18 mo old and ranged in body length from 5 to 30 cm. Wheat germ agglutinin was received from E. Y. Laboratories, Inc. (San Mateo, CA). Purified collagenase (CLSS 130 U/mg) was purchased from Worthington Biochemical Corp. (Freehold, NJ) and purified hyaluronidase (type 1-S, 290 U/mg) from Sigma Chemical Co. (St. Louis, MO).

Retinal Dissociation and Cell Plating

Fish were dark-adapted for 1–2 h and, in complete darkness, were then anesthetized by cold, decapitated, and pithed. Under infrared illumination, aided by a TV camera and monitor, an eye was enucleated and hemissected and the retina was isolated in a fish saline solution of composition (mM): 136 NaCl, 2.4 KCl, 5 $NaHCO_3$, 1 NaH_2PO_4, 1 $MgCl_2$, 1 $CaCl_2$, 10 glucose, and 10 HEPES, pH 7.5, osmotic pressure 309 mosM. The isolated retina was cut into halves and incubated for 10 min in the saline solution supplemented with collagenase and hyaluronidase, each at a concentration of 0.4 mg/ml. After incubation, the retina sections were washed free of enzymes and glucose by transferring them successively through three 10-ml rinses of fish saline in which glucose was isosmotically replaced by 5 mM Na-pyruvate. The retina sections were further cut into three to five pieces, and one of these pieces was transferred to 800 μl of the pyruvate saline, where it was shredded using fine forceps. 200 μl of the resulting cell suspension, free of retinal fragments, was transferred onto a wheat germ agglutinin–coated glass coverslip produced with 5 mg/ml lectin as described by Cherr and Cross (1987). This coverslip was on the bottom of a shallow chamber designed for electrophysiological recordings. We allowed 15–20 min for cells to settle and adhere to the coverslip in the recording chamber and we then exchanged the incubation solution with standard fish saline containing glucose. Cells could be stored in the dark at 7–8°C in fish saline for up to 4 h preceding electrical recordings.

Electrical Recordings

The electrophysiological recording chamber was held on the stage of an upright microscope equipped with DIC optics. Cells were observed under visible light. We recorded currents from excised membrane patches using tight-seal electrodes (Hamill, Marty, Neher, Sakmann, and Sigworth, 1981) fabricated from Corning 1724 glass (aluminosilicate, 1.5:1.0 mm o.d./i.d.) with typical tip openings of 0.4–0.8 μm (resistance 5–8 MΩ when filled with standard extracellular solution). We attained seals ranging in resistance between 1 and 10 GΩ by applying the tight-seal electrodes onto the distal third of cone outer segment, most often on the side of the cell but occasionally at the tip. We obtained excised, inside-out membrane patches by rapidly withdrawing the electrode from the outer segment surface after forming a giga-seal. For reasons that remain unexplained, some cells (~20%) yielded patches that were unresponsive to cGMP, perhaps because of formation of closed membrane vesicles or outside-out patches. To maintain cell health, we operated under dim red or blue light and minimized exposure of the cells to the illuminator in the microscope.

We measured membrane currents under voltage clamp at room temperature (22–23°C) using a patch-clamp amplifier (EPC-7; List Instruments, Darmstadt, Germany). We compensated for the membrane and electrode capacitance, but because current amplitude was generally small we did not compensate for series resistance. The analog signal was filtered at 1,500 Hz with an 8-pole, low pass Bessel filter (Frequency Devices Inc., Haverhill, MA) and digitized on-line with 12-bit accuracy at a 5-kHz acquisition rate (DT 2782; Data Translation, Marlboro, MA). Signal acquisition and membrane voltage were under microcomputer control (PDP 11/23; DEC, Maynard, MA). As is conventional, currents flowing from the cytoplasmic to the extracellular surface of the detached patch were referred to as outward in direction and assigned positive values; membrane voltage was defined under the convention that the extracellular surface was at ground potential. Curve fitting in data analysis was executed using a nonlinear, least-squares minimization algorithm (NFIT; Island Products, Galveston, TX). Simulations to fit the *I-V* curves were executed in a computer using MathCAD software (MathSoft, Cambridge, MA).

Perfusion Procedures and Solutions

The recording chamber was ~ 1 ml in volume and was intermittently perfused with fish saline at a rate of ~0.5 ml/min. We attained seals and produced detached membrane patches from cones held in the main compartment of this chamber. After patch excision we slowly moved the tight-seal electrode, under solution, from the main compartment to a smaller compartment that could be separated from the rest of the chamber by a movable gate. The gate prevented exposure of intact cells to the solutions used to test the detached membrane patch. A reference electrode was connected to the smaller compartment via a 1 M KCl/agar bridge. In the small compartment, we placed the tip of the tight-seal electrode within 150 μm of the opening of a 100-μm-diam glass capillary. Test solutions, selected with a rotary valve, flowed out of this capillary tube at a rate of ~0.6 ml/min. At this flow rate, the solution bathing the membrane patch was fully exchanged within 30 s of a change in position of the selection valve; however, we commenced recordings of membrane currents 60 s after solution changes. In a typical experiment, we first measured membrane currents in the normal fish saline in the absence of cGMP. We returned to this initial condition after each presentation of the various solutions tested in a given membrane patch. For a given patch we accepted data for further analysis only if the electrical characteristics of the membrane, when returning to the initial conditions, changed by < 10% over the course of the measurements.

The extracellular surface of the detached membrane patch was bathed by the pipette filling solution, whose composition in all experiments was (mM): 157 NaCl, 1 EGTA, 1 EDTA, and 10 Na-HEPES, pH 7.5, osmotic pressure 305 mosM. As the initial condition in all experiments the cytoplasmic (outside) membrane surface was bathed with the same solution. In the course of measurements we changed the composition of the solution bathing the intracellular membrane surface. In general, the composition of test solutions was one of three types: (*a*) Solutions with the initial composition, but containing varying concentrations of cGMP in the range between 10 and 800 μM. (*b*) Solutions with the initial composition containing 200 μM cGMP and in which NaCl was entirely replaced with 157 mM of KCl, RbCl, CsCl, LiCl, or tetramethylammonium (TMA), or with 174 mM arginine. In each of these solutions pH was titrated with the hydroxide form of the monovalent cation. (*c*) Solutions with the initial composition containing 200 μM cGMP and in which NaCl was replaced by NaCl or LiCl at various concentrations ranging between 5 and 500 mM. Because we used a 1 M KCl agar bridge with the reference electrode, changing test solutions caused only small changes in the junction potential at this electrode; nonetheless, we measured the junction potential for each solution tested and corrected command voltages by this value.

Measurement of Ion Permeabilities

We measured reversal potentials under bi-ionic conditions, V_{rev}, by determining the potential at which membrane current was zero in amplitude. Ionic permeability of ion C, relative to the permeability of sodium (P_c/P_{Na}), was calculated from the difference between the reversal potential measured under symmetric Na solutions and the reversal potential measured when Na on the cytoplasmic membrane surface was replaced by the same concentration of ion C (Hodgkin and Katz, 1949):

$$\frac{P_c}{P_{Na}} = \frac{[Na]_o}{[C]_i} \exp\left(\frac{-F\Delta V_{rev}}{RT}\right) \quad (1)$$

where R, T, and F have their usual meanings. ΔV_{rev} is the difference in reversal potentials, $[Na]_o$ is the activity of Na at the external membrane surface (121 mM), and $[C]_i$ is the activity of cation C at the cytoplasmic surface. Ionic activities were calculated from concentrations using activity coefficient tables (Robinson and Stokes, 1965).

RESULTS

Mechanical dissociation of the retina of striped bass yielded isolated rod and cone photoreceptors that were easily identified by their characteristic anatomy. We further identified cone photoreceptors as either single or twin. The cone photoreceptors were not anatomically complete: they consisted of the outer segment and part of the inner segment (ellipsoid and myoid) but lacked the nuclear region and synaptic pedicle. These solitary cones, nonetheless, remained viable for several hours, and under appropriate conditions their phototransduction signals were indistinguishable from those measured in the intact retina.[1] We excised inside-out membrane patches from the distal third of the outer segment, most frequently from the side but also from the tip (~40% of patches). We did not find systematic differences in the electrical properties of membrane patches as a function of either cone type or spatial site of origin. Thus, the data we present here are the sum of our results and indicate that the same ion channels are present throughout the plasma membrane in the distal third of single and twin cone outer segments.

cGMP-dependent Currents in Outer Segment Membrane Patches

Studies of light transduction in bass cones have shown that the outer segment membrane contains only one class of ion channels, those regulated by light and gated by cGMP.[1] Indeed, detached membrane patches under symmetric NaCl solutions free of divalent cations and in the absence of cGMP exhibited extremely high resistance, in the range of 3–5 GΩ. Addition of cGMP to the cytoplasmic (outside) surface of the membrane patches reversibly activated ionic currents (Fig. 1). We measured the properties of these currents as a function of membrane voltage. In our analysis, we defined the cGMP-gated currents as the difference between the currents generated by applied steps of voltage in the presence and absence of the nucleotide. The maximum current amplitude measured at +80 mV under symmetric NaCl solutions and in the presence of saturating cGMP concentrations ranged between 63 and 2,318 pA (average = 975.9, n = 34). When outward current amplitude was large (e.g., at depolarizing voltages above +60 mV and in the presence of saturating cGMP

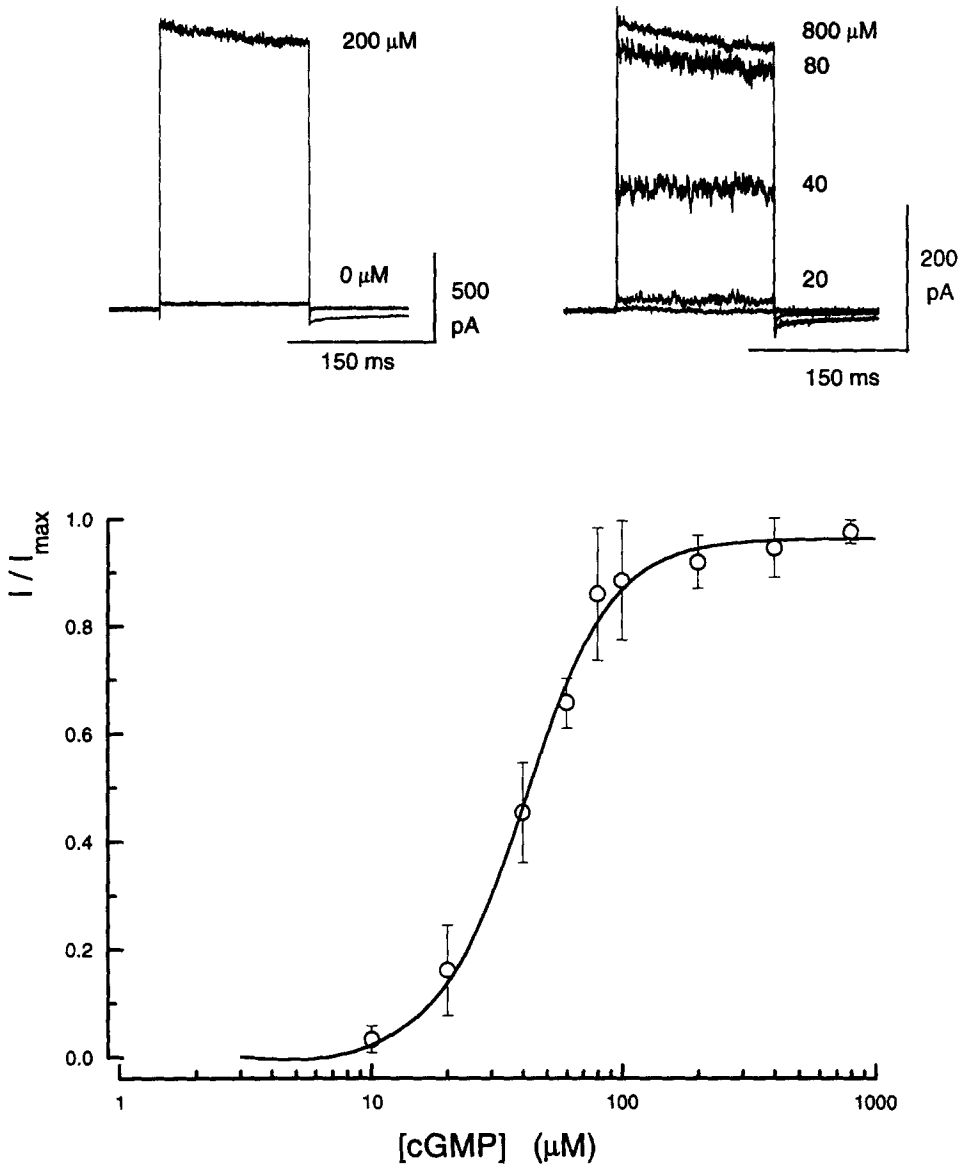

FIGURE 1. cGMP dependence of current amplitude in detached cone outer segment membranes. Currents illustrated in the top panels were measured in the same inside-out membrane patch in the presence of symmetric NaCl solution. The top left panel illustrates currents measured in response to 150-ms voltage steps to +80 mV before, during, and after the application of 200 μM cGMP onto the cytoplasmic surface of the patch. The currents before and after cGMP cannot be distinguished from each other. The top right panel illustrates currents measured in response to 150-ms voltage steps to +80 mV in the presence of cGMP at concentrations that ranged between 20 and 800 μM. The lower panel illustrates the dependence of current amplitude on cytoplasmic cGMP concentration. The data points are the average (±SD) of normalized current amplitudes measured at +80 mV in four patches. The continuous line is the Hill equation (Eq. 2) fit to the data by a nonlinear least-squares algorithm. Optimum fit was obtained with average values of K_{cGMP} = 42.6 ± 5.9 μM (±SD) and n = 2.49 ± 0.79 (±SD).

concentrations), in ~40% of the patches we observed a time-dependent sag in current amplitude (for example, see Fig. 6); under all other conditions the cGMP-dependent current was time invariant. In our analysis, when time dependence was apparent we measured the maximum current amplitude 2–5 ms after the voltage step. Zimmerman, Karpen, and Baylor (1988) have shown in rod membrane patches that this time dependence is not a feature of ion channel activity; rather, it is a consequence of ion depletion near the membrane surface.

The amplitude of the cGMP-gated currents was a function of cGMP concentration (Fig. 1). To quantify this dependence and compare results among all patches, we normalized the data by dividing current amplitude at each cGMP concentration by the maximum amplitude measured in that patch. The dependence of current amplitude on cGMP concentration was well described by the Hill equation (Fig. 1):

$$\frac{I(\text{cGMP})}{I_{\max}} = \frac{[\text{cGMP}]^n}{[\text{cGMP}]^n + K_{\text{cGMP}}^n} \tag{2}$$

where $I_{\max}$ is the maximum current, I(cGMP) is the current amplitude measured at a cGMP concentration given by [cGMP], K_{cGMP} is that concentration at half-saturating current amplitude, and n is a coefficient that indicates cooperative interaction in the activation of current. At +80 mV, the average values estimated from optimized fits to data from four patches were: K_{cGMP} = 42.6 ± 5.9 μM (±SD) and n = 2.49 ± 0.79 (±SD).

I-V Characteristics of cGMP-gated Currents

The binding constant of cGMP to the cone outer segment channels, K_{cGMP}, was weakly voltage dependent. Fig. 2 illustrates the cGMP dependence of current amplitude measured at +50 and −50 mV. At +50 mV K_{cGMP} = 43.4 μM and at −50 mV K_{cGMP} = 33.6 μM. This difference has an important physiological consequence: in a given patch the *I-V* curve of the cGMP-gated currents measured under symmetric ionic solutions exhibited rectification at nonsaturating cGMP concentrations that was absent at saturating cGMP concentrations (Fig. 3). The rectification may arise in part from the fact that under nonsaturating conditions, as membrane voltage hyperpolarizes, the effectiveness of cGMP as an activator decreases. Thus, it would be expected that membrane conductance would decrease as potential hyperpolarizes. This we indeed observed in the range between −50 and +80 mV. However, at voltages more hyperpolarized than −50 mV the membrane conductance increased as the potential hyperpolarized. The mechanism of this increase is unknown, but it cannot be explained by the voltage dependence of K_{cGMP}.

In the absence of divalent cations and the presence of cGMP concentrations that saturate current amplitude, the amplitude of the cone outer segment currents were linearly dependent on voltage over the range between −80 and +80 mV (Fig. 3). However, the curves exhibited rectification in the presence of Ca ions: if Ca was added to one side of the membrane, regardless of which side, the conductance became voltage dependent. In the presence of Ca ions, the *I-V* curves of the cGMP-gated currents were well fit by an empirical equation that has been extensively used in the past to described the voltage dependence of the light-sensitive currents in

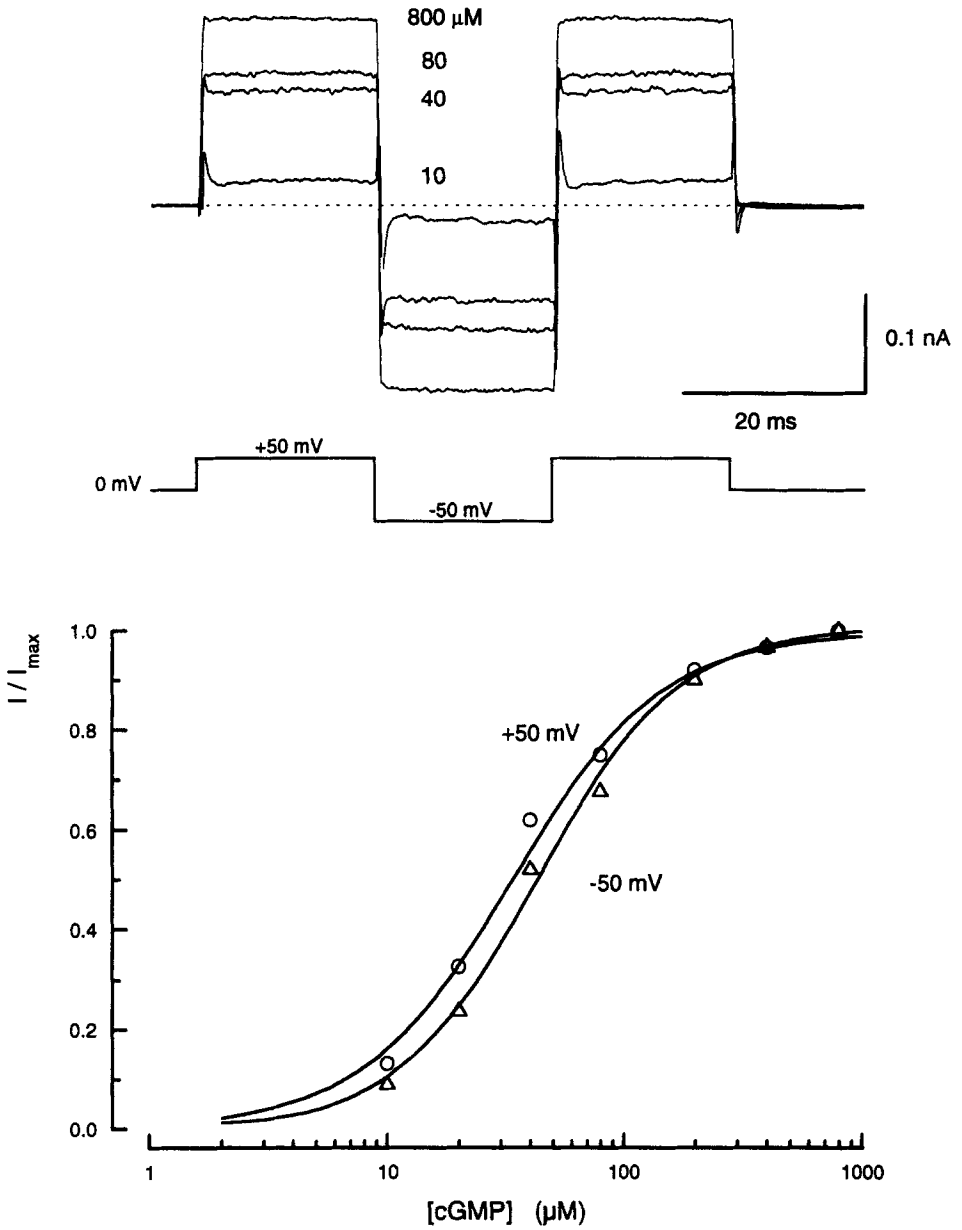

FIGURE 2. Effect of voltage on the cGMP dependence of current amplitude in cone outer segment membranes. The upper panel illustrates currents measured in the same patch, under symmetric NaCl solutions, in response to voltage steps to +50 and −50 mV as shown. Current measurements were repeated in the presence of cGMP at various concentrations in the range between 20 and 800 μM. The lower panel illustrates the dependence of normalized current amplitude on cytoplasmic cGMP concentration. The continuous line is the Hill equation (Eq. 2) fit to the data by a nonlinear least-squares algorithm. Optimum fit was obtained with the values K_{cGMP} = 43.4 μM and n = 1.36 at −50 mV and K_{cGMP} = 33.6 μM and n = 1.45 at +50 mV.

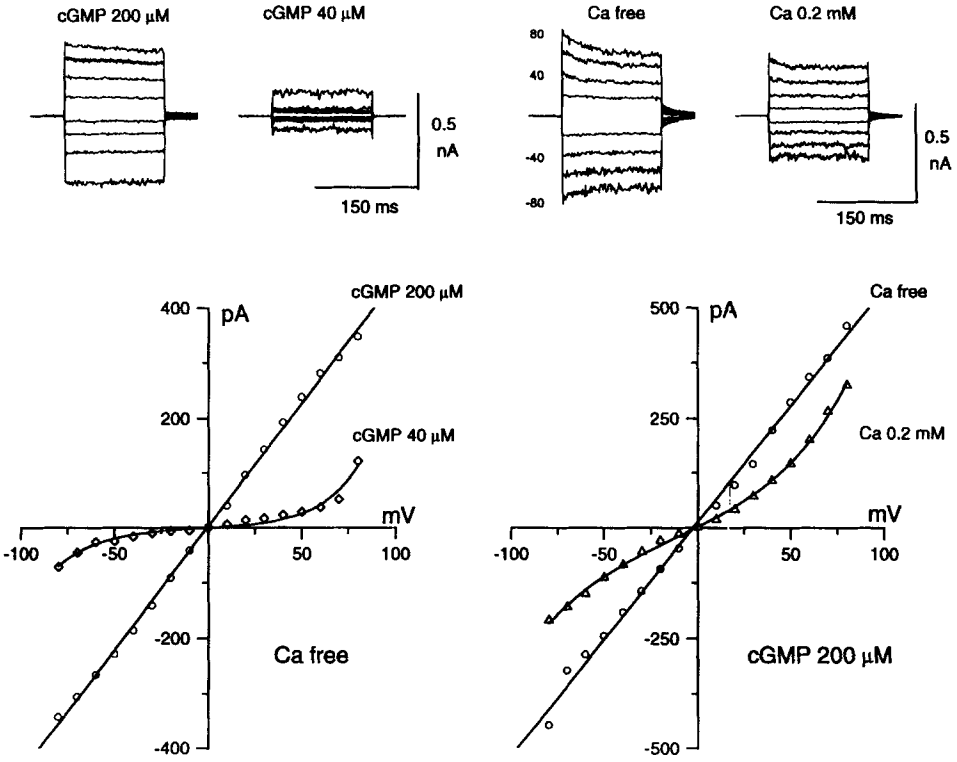

FIGURE 3. *I-V* curves of cGMP-gated currents in cones. On the left, upper panels show currents measured in the presence of symmetric NaCl and chelators of divalent cations (EGTA and EDTA) in response to 150-ms voltage steps in the range between −80 and +80 mV, covered in 20-mV increments. We illustrate difference currents measured in the same patch before and after the application of either 40 or 200 μM cGMP. The continuous line in the *I-V* plots at 200 μM cGMP is straight, but at 40 μM it is the best fit to the data of Eq. 3 with values $A_1 = 2.21$, $A_2 = 2.48$, $V_r = -0.7$, $V_o = 11$, and $\gamma = 0.46$. On the right, upper panels show currents measured in the presence of symmetric NaCl in response to 150-ms voltage steps in the range between −80 and +80 mV, covered in 20-mV increments. The currents displayed are the difference, at each voltage, of the currents measured before and after the application of 200 μM cGMP onto the cytoplasmic membrane surface. We show currents measured in the same patch either in the absence of divalent cations or with 0.2 mM Ca present on the cytoplasmic surface. The continuous lines in the *I-V* plots are either straight, in the absence of divalent cations, or the best fit to the data of Eq. 3, in the presence of Ca. Optimum fit was obtained with the values $A_1 = 32.9$, $A_2 = 65.8$, $V_r = -16.8$, $V_o = 23$, and $\gamma = 0.44$.

photoreceptors (reviewed in Yau and Baylor, 1989):

$$I(V) = A_1 \exp\left((1-\gamma)\frac{(V-V_r)}{V_o}\right) + A_2 \exp\left((-\gamma)\frac{(V-V_r)}{V_o}\right) \quad (3)$$

where A_1 and A_2 are adjustable current amplitudes and V_r, V_o, and γ are adjustable parameters. Nonlinear, least-squares fits of the model to data for 10 patches under symmetrical Ca (0.2 mM) solutions had the following average values (±SD): $\gamma = 0.47$

(±0.03), V_r = −0.5 mV (±4.7), and V_o = 17.49 (±0.09). The same function with similar values for the adjustable parameters describes well the *I-V* curve of the light-sensitive currents in intact bass cones.[1]

Permeability and Conductance Sequence of Monovalent Cations

We conducted all studies of monovalent cation permeability in the absence of divalent cations (with added EDTA [1 mM] and EGTA [1 mM]). cGMP-gated channels are impermeant to monovalent anions. In five different patches we observed no change at all in the reversal potential of cGMP-gated currents measured in the presence of symmetrical NaCl solutions when compared with those measured when NaCl on the cytoplasmic side of the membrane was replaced by the same concentration of Na-isethionate (data not shown). Also, the Nernst equation calculated for ideal selectivity of cations over anions accurately described the dependence of reversal potentials of the cGMP-dependent currents on NaCl concentration gradients (see Fig. 10). To determine the permeability sequence among monovalent cations, we measured zero current potentials under bi-ionic gradients. The extracellular surface of a patch was bathed with 157 mM NaCl, while the intracellular surface was sequentially bathed with solutions containing 200 μM cGMP and 157 mM of LiCl, KCl, RbCl, or CsCl. Fig. 4 illustrates typical voltage-clamped current records and *I-V* curves measured in the same patch under the various bi-ionic solutions. The average permeability constants calculated from data collected in 10 different patches were:

$$P_K : P_{Na} : P_{Li} : P_{Rb} : P_{Cs}$$
$$1.11 : 1.0 : 0.99 : 0.96 : 0.8$$

To investigate ionic selectivity as reflected in membrane conductance, we measured *I-V* curves over the range of −80 to +80 mV under bi-ionic gradients in the presence of saturating cGMP concentrations (Fig. 5). To compare results among patches, we normalized the data in each patch by dividing the current amplitude measured at each voltage in each solution by the amplitude of the current measured under symmetric NaCl solutions at absolute +80 mV. Outward currents, carried by the various cations tested, increased in amplitude linearly with depolarizing voltages. The average selectivity sequence determined from the conductance ratios for the outward currents at absolute +80 mV from eight different patches was:

$$G_{Na} : G_K : G_{Rb} : G_{Cs} : G_{Li}$$
$$1.0 : 0.99 : 0.88 : 0.74 : 0.60$$

We measured the same sequence, with minor differences in the ratios for Rb and Li, at absolute +40 mV:

$$G_{Na} : G_K : G_{Rb} : G_{Cs} : G_{Li}$$
$$1.0 : 0.99 : 0.91 : 0.74 : 0.66$$

Under bi-ionic gradients inward currents were carried by Na ions, regardless of the ionic species on the cytoplasmic surface of the membrane. It would be expected, therefore, that the inward currents would be essentially identical under all bi-ionic conditions if the flow of cations in one direction is not significantly affected by the

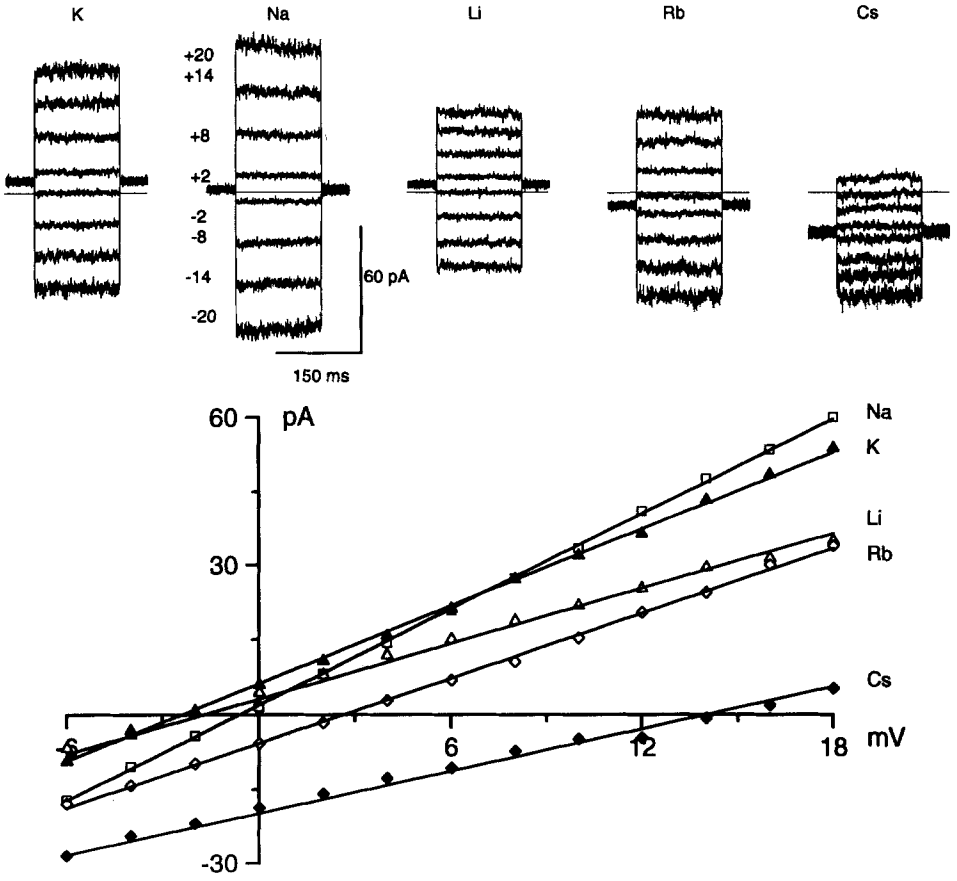

FIGURE 4. Selectivity of the cGMP-gated channels in cones for monovalent cations. The upper panels illustrate currents measured in the same membrane patch in response to 150-ms voltage steps in the range between −20 and +20 mV covered in 6-mV increments. For each ion we show difference currents measured before and after application of 200 μM cytoplasmic cGMP. The extracellular membrane surface was bathed with 157 mM NaCl. The cytoplasmic surface was bathed with 157 mM of each cation tested. In the current records, the continuous straight line indicates the zero current level. The continuous lines in the *I-V* plot are cubic spline lines best fit to the data points. The membrane voltage at zero current was interpolated from the continuous lines in order to calculate ion permeabilities.

chemical identity of the ions on the opposite side of the membrane. Indeed, within experimental error, inward currents were identical under all bi-ionic solutions. Similar results were reported for rod membranes by Menini (1990), but not by Furman and Tanaka (1990).

Permeability of Organic Cations

To investigate the importance of steric factors in cation selectivity we tested the permeability of two organic cations of dissimilar crystal radius: TMA (radius: 2.6 Å)

and arginine (radius: 5.3 Å). We measured membrane currents at various voltages in the presence of 200 μM cGMP under bi-ionic gradients where 157 mM NaCl on the cytoplasmic surface was isosmotically replaced by either 157 mM TMA-Cl or 174 mM arginine-Cl. To compare results among patches, we normalized currents by dividing the amplitude measured at each voltage and each ion tested by that measured under symmetric NaCl solutions at +80 mV in the same patch. TMA was essentially impermeant since no outward current or reversal potential could be measured in its

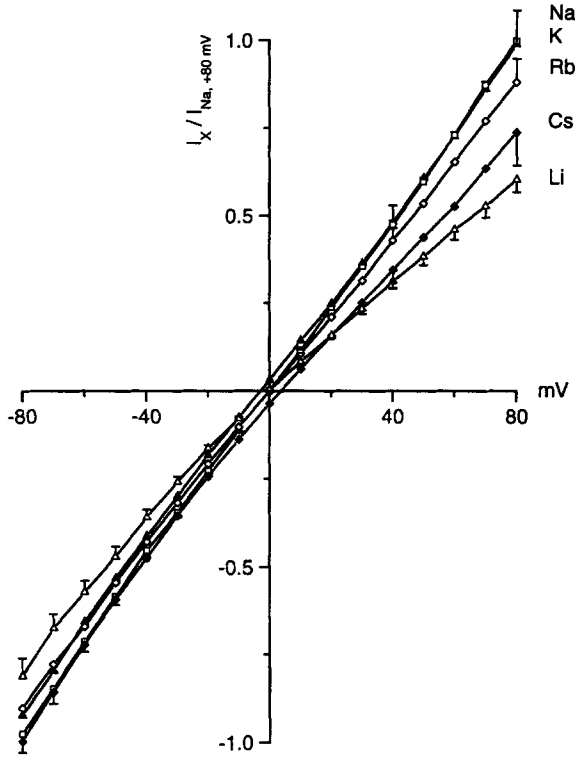

FIGURE 5. Conductance sequence among monovalent cations in the cGMP-gated channels of cones. Measurements were conducted under bi-ionic conditions with NaCl on the extracellular membrane surface and the same activity of each of the various test cations in the cytoplasmic surface. Data points in the *I-V* plot are the average of normalized current amplitude measured in 10 different patches in the presence of 200 μM cytoplasmic cGMP. Current amplitude was normalized for each cation by dividing it by the amplitude measured under symmetric NaCl solutions at +80 mV in the same patch. Error bars are SEM. For graphical clarity we display error bars at all voltages for Na and Li, while for the other ions we display error bars only at +40 and +80 mV, the values used to calculate the sequences given in the text. The lines joining the data points were drawn by hand.

presence (Fig. 6). Arginine, on the other hand, was permeable to a limited extent: it sustained a small outward current and its zero current reversal potential indicated a permeability ratio, $P_{arg}/P_{Na} = 0.25$ ($n = 3$) (Fig. 6). It is important to note, however, that both organic cations not only reduced or abolished the outward current that they carried, but also reduced the inward current carried by Na. This blocking effect of TMA or arginine was fully reversible (Fig. 6). Thus, TMA is impermeant, arginine permeates to a limited extent through the cGMP-gated channels, and both significantly block the open channels.

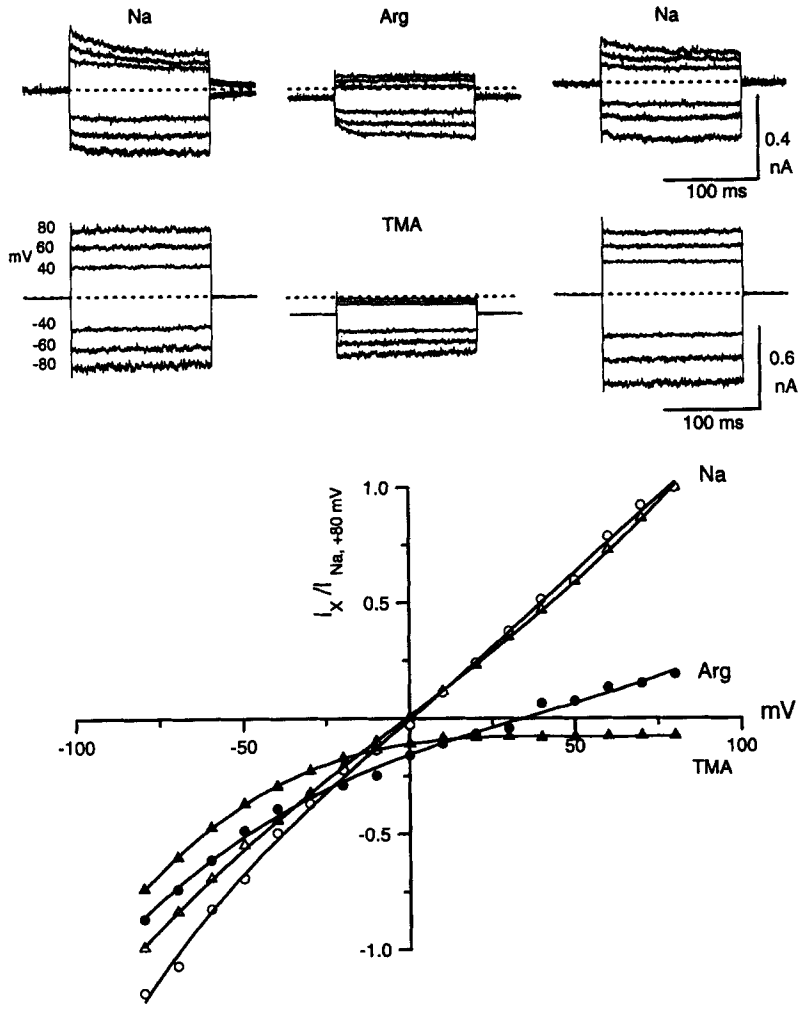

FIGURE 6. Permeation of organic cations through the cGMP-gated channels of cones. Each of the upper panels shows currents activated by voltage steps to ±40, ±60, and ±80 mV. The currents shown are the difference measured before and after application of 200 μM cytoplasmic cGMP. Indicated as a dotted line is the zero current value for each set of traces. The data shown in the upper and lower current panels were collected in different membrane patches. In each patch, we compared currents measured in symmetric 157 mM NaCl with those measured in bi-ionic solution with the same NaCl on the outside surface and either 174 mM arginine (upper current traces) or 157 mM TMA (lower current traces) on the cytoplasmic surface. The blocking effects of organic cations were fully reversible since currents in symmetric NaCl solutions were the same before and after application of the organic cations. Under the initial ionic conditions, the currents in the membrane patch illustrated in the uppermost records exhibited a time-dependent relaxation at large depolarization. Such relaxation was absent in the patch illustrated in the lower records. The relaxation is not a molecular property of the channel, but a consequence of ion depletion in the unstirred space near the membrane (Zimmerman et al., 1988), which varies among patches. In the *I-V* plots, currents were normalized by dividing their amplitude under each test solution by the amplitude of the current under symmetric NaCl at +80 mV measured in the same patch. The continuous lines in the *I-V* plots were drawn by hand. Open symbols identify the *I-V* curves measured before the application of each of the organic cations. Circles identify data from the patch tested with arginine, while triangles identify the data from the patch tested with TMA. The *I-V* curves upon returning to the initial conditions were essentially identical to those first measured and shown.

Dependence of Permeation Properties on Ion Concentration

The selectivity sequence we measured suggests the presence in the cone cGMP-gated channel of a strong field strength site that binds cations as they permeate through the channel (Eisenman and Horn, 1983). To explore the features of this cation binding site in the channels, we measured the amplitude of outward currents as a function of cation concentration on the cytoplasmic surface of the membrane. The extracellular membrane surface was bathed with 157 mM NaCl, while cytoplasmic concentration changed over the range of 5–500 mM in the presence of 200 μM cGMP. Fig. 7 illustrates currents and *I-V* curves measured in varying cytoplasmic NaCl, while Fig. 8 illustrates similar data measured in varying cytoplasmic LiCl concentrations. For both cations, at large depolarizing voltages, the amplitude of the outward currents increased with ion activity. To compare results among patches, we normalized the data by dividing current amplitude at each voltage and each concentration by that measured at +80 mV with 157 mM cytoplasmic NaCl in the same patch. The dependence at +80 mV of the amplitude of outward currents on cytoplasmic ion concentration, for both Na and Li, is illustrated in Fig. 9. Experimental data were well described by the Langmuir adsorption isotherm for a single ion binding site (Fig. 9):

$$\frac{I(c)}{I_{max}} = \frac{[c]}{K_s + [c]} \tag{4}$$

where $I(c)$ is the current amplitude at ion activity [c], I_{max} is the saturated current amplitude, and K_s is the equilibrium constant of the binding site. This method of analysis is only applicable at large values of membrane voltage, when unidirectional current amplitude is expected to be limited by ion concentration (Hille, 1984). The values of the equilibrium constant K_s were voltage dependent, a feature that is well explained by the model of the ion channel discussed in detail below. At +80 mV the average value of K_s for Na was 104 mM (±8.85 SD, n = 14), while for Li it was 37.6 (±4.71 SD, n = 6) (Fig. 9).

FIGURE 7. (*opposite*) Effects of cytoplasmic Na concentration on cGMP-gated currents. We illustrate the currents measured with the external membrane surface bathed in 157 mM NaCl and the cytoplasmic surface bathed in NaCl at various concentrations in the range between 5 and 500 mM, as indicated. The dotted straight line in the current records denotes the zero current level. In the *I-V* plot, the data points are (in units of concentration): 5 mM (*diamonds*), 25 mM (*squares*), 50 mM (*triangles*), 157 mM (*filled circles*), and 500 mM (*open circles*). The continuous lines in the *I-V* plot were calculated theoretically for the known ion activity gradient according to the single site, double barrier model of the channel described in the text and the Appendix. From the best fit between model and experimental data, the average height of the energy barriers and troughs and their location in the channel were (see Fig. 12 for definition of terms): $G_1 = G_3 = 0$; $G_{12} = 11.44\ RT$ (±0.10 SD, range = 11.38–11.6); $G_2 = -5.13\ RT$ (±0.07 SD, range = −5.05–−5.22); and $G_{23} = 9.8\ RT$ (±0.18 SD, range = 9.6–10). Also, $d_{12} = 0.15$, $d_2 = 0.5$, and $d_{23} = 0.76$.

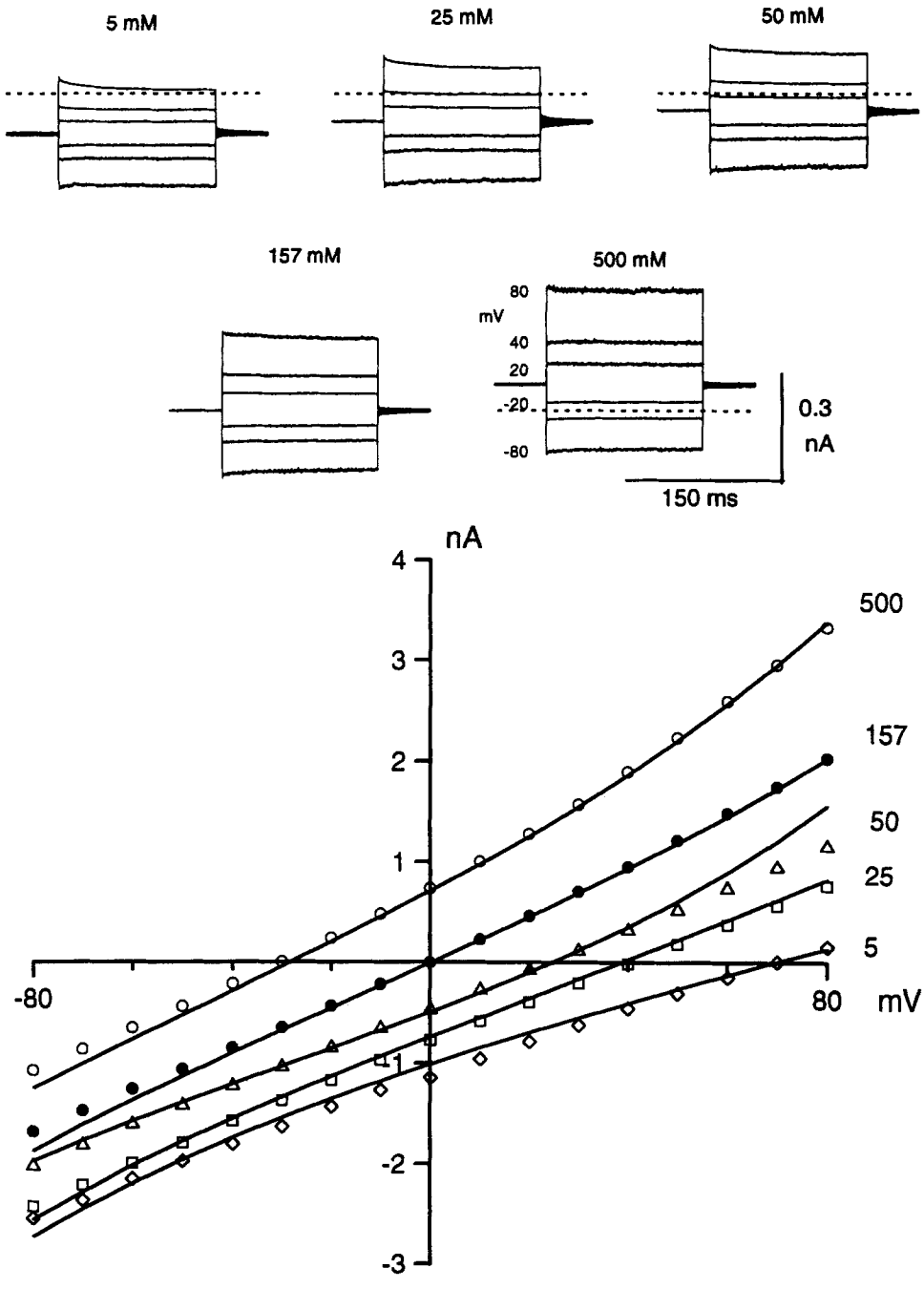
5 mM
25 mM
50 mM
157 mM
500 mM
80
mV
40
20
-20
-80
0.3
nA
150 ms
nA
4
3
2
1
-1
-2
-3
500
157
50
25
5
-80
80
mV

FIGURE 7.

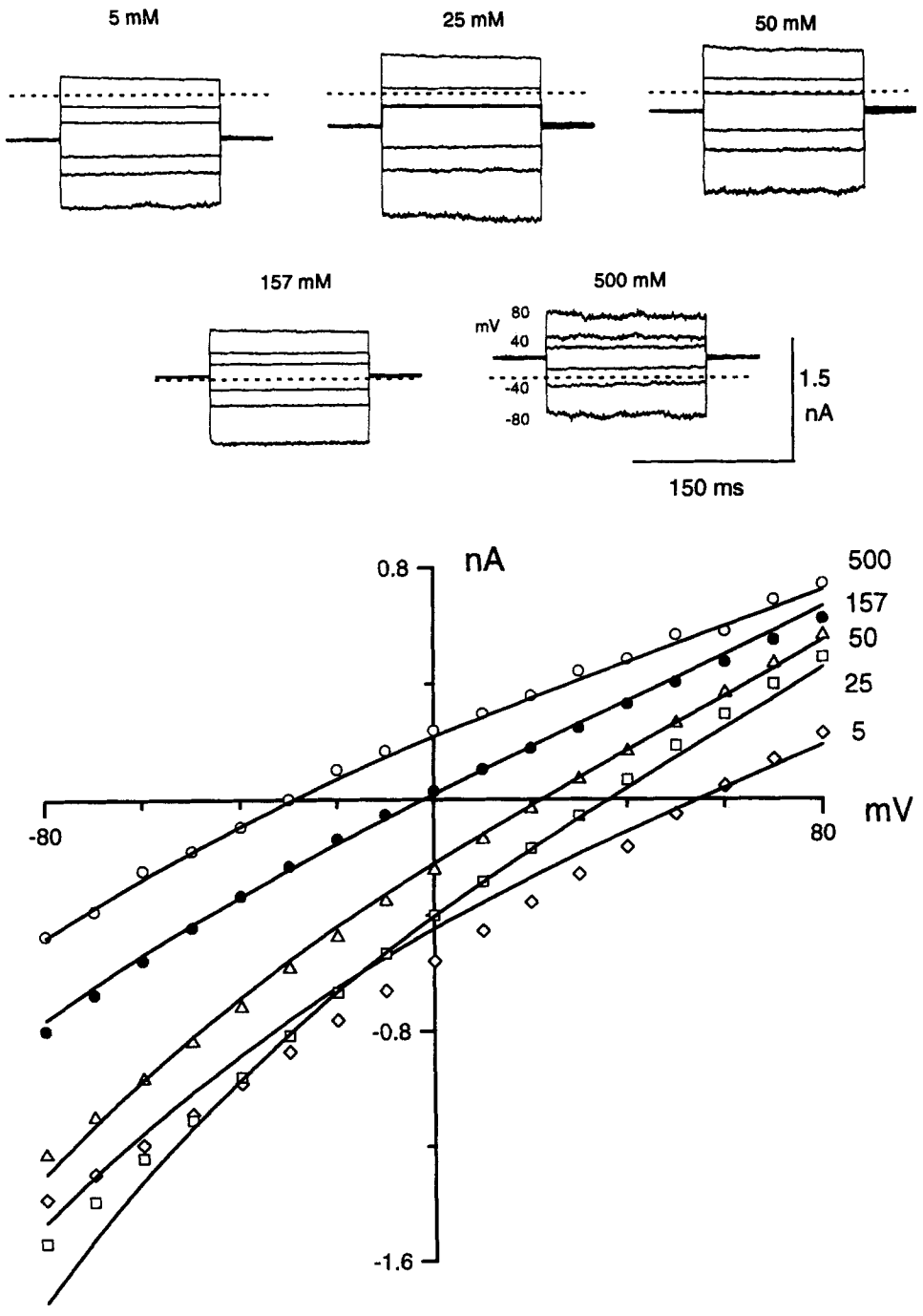
5 mM
25 mM
50 mM
157 mM
500 mM
mV
80
40
-40
-80
1.5
nA
150 ms
nA
0.8
-0.8
-1.6
-80
80
mV
500
157
50
25
5

FIGURE 8.

Dependence of I-V Curves on Ion Concentration

The reversal potential of the cGMP-dependent currents for both NaCl and for LiCl shifted as we changed the ion concentration gradient across the membrane (Figs. 7 and 8). An analysis of the dependence of this reversal potential on ion concentration is the most sensitive method for defining the anion to cation selectivity of the channel. Analysis of the results obtained in 14 patches in the case of NaCl and 6 patches for LiCl is shown in Fig. 10. The continuous line in this figure is the best fit to the data. The reversal potential for both Na and Li changed linearly with the logarithm of the ion activity with a slope of 57.9 mV/decade (±3.1 SD) for Na and 53.2 mV/decade (±2.3 SD) for Li. This essentially ideal Nernstian behavior reveals that the cGMP-gated channels are extremely selective for cations over anions.

The nonlinear dependence of current amplitude on ion concentration and the fact that it reached a saturating value (Fig. 9) demonstrate that monovalent cations do not cross the cGMP-gated channels independently of each other (Hille, 1984). Current saturation and the failure of independence can be explained theoretically by a model that assumes that the ion channel contains discrete cation binding sites that are separated from each other and from the surfaces of the membrane by a series of energy barriers. In this model, first described by Eyring, Lumry, and Woodbury (1949) and discussed in detail by Lauger (1973) and Hille (1975*a*, *b*), ion flux is seen to arise from the crossing of the discrete energy barriers at rates defined by the energy differences across the barriers (Fig. 12 in the Appendix). In the presence of membrane voltages, the energy barriers are defined both by a chemical term that characterizes the interaction of the ion with sites within the channel, and an electrostatic term that defines the effects of membrane voltage. This model allows quantification of the competition observed when two permeant ions are simultaneously present. In the Appendix we briefly detail the method we used to apply this theory to the analysis of the cGMP-dependent currents. In our analysis we assumed the simplest form of the model, one in which the cGMP-gated channel contains a single ion binding site that is separated from each membrane surface by one energy

FIGURE 8. (*opposite*) Effects of cytoplasmic Li concentration on cGMP-gated currents. The panels show currents activated by voltage steps in the range between −80 and +80 mV in 40-mV increments. The currents shown are the differences measured before and after application of 200 μM cytoplasmic cGMP. The data shown were all collected in the same patch. We illustrate the currents measured with the external membrane surface bathed in 157 mM NaCl and the cytoplasmic surface bathed in LiCl at various concentrations in the range between 5 and 500 mM, as indicated. The dotted straight line in the current records denotes the zero current level. In the *I-V* plot the data points are (in units of concentration): 5 mM (*diamonds*), 25 mM (*squares*), 50 mM (*triangles*), 157 mM (*filled circles*), and 500 mM (*open circles*). The continuous lines in the *I-V* plot were calculated theoretically for the known ion activity gradient according to the single site, double barrier model of the channel described in the text and the Appendix. From the best fit between model and experimental data, the average height of the energy barriers and troughs and their location in the channel can be (see Fig. 12 for definition of terms): $G_1 = G_3 = 0$; $G_{12} = 10.38\ RT$ (±0.10 SD, range = 10.20–10.45); $G_2 = -5.57\ RT$ (±0.06 SD, range = −5.52–5.68); and $G_{23} = 10.09\ RT$ (±0.17 SD, range = 9.9–10.29). Also, $d_{12} = 0.3$, $d_2 = 0.5$, and $d_{23} = 0.65$.

barrier (Fig. 12). We assumed the binding site was located in the middle of the membrane, but we allowed the barrier peaks to adopt asymmetric positions with respect to the center. We further assumed that the binding site was occupied by only one ion at a time.

This simple double barrier, single ion, single binding site model successfully simulated the *I-V* curves we measured experimentally, both for currents in the

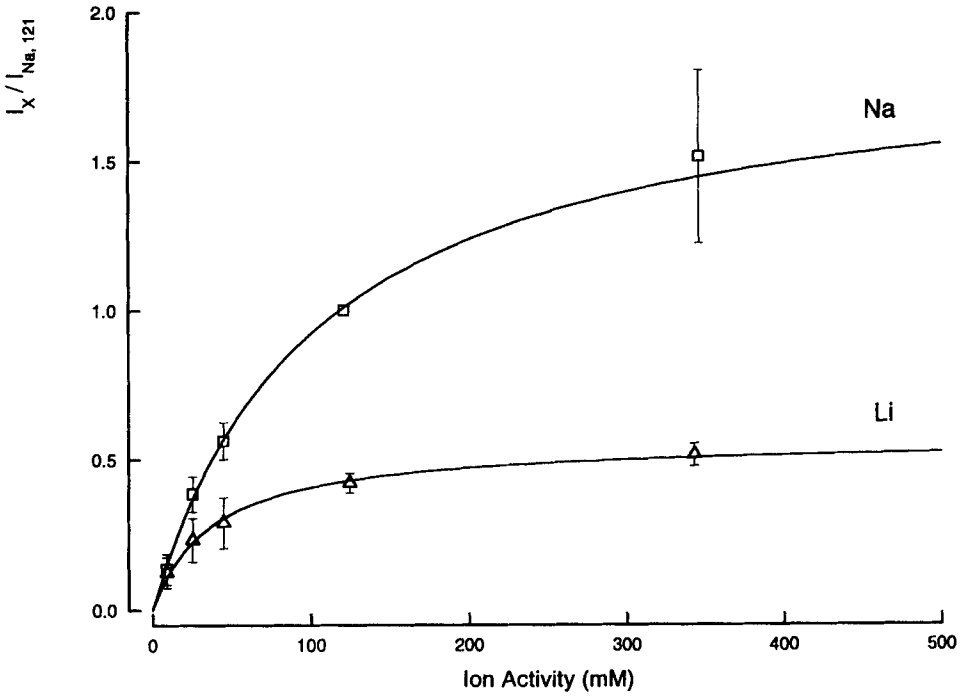

FIGURE 9. Dependence of the amplitude of cGMP-gated outward current on the cytoplasmic concentration of Na or Li at +80 mV. We measured currents activated by 200 μM cGMP in membrane patches bathed with 157 mM NaCl on the external surface and varying concentration of NaCl or LiCl on the cytoplasmic surface. To compare data among patches, outward currents at +80 mV were normalized by dividing their amplitude at each concentration by that measured at +80 mV under symmetric NaCl solution in the same patch. The abscissa indicates concentration in units of activity. The data points are the average (±SD) of data from 14 patches for NaCl (*squares*) and 6 patches for LiCl (*triangles*). The continuous lines are least-squares best fits to the data of the Langmuir adsorption isotherm (Eq. 4). Optimum fits were obtained with K_s values for NaCl of 104 mM (±8.85 SD) and for LiCl of 37.6 (±4.71 SD).

presence of NaCl concentration gradients (Fig. 7) and bi-ionic Na-Li concentration gradients (Fig. 8). We found that asymmetric energy barriers provided the best fits between model and experimental data. The features of the energy barriers that best fit our data are detailed in the legends to Figs. 7 and 8. This model also described well the dependence on membrane voltage of the value of K_s, both for Na and for Li. As expected, the depth of the energy well was larger for Li than for Na, since Li

appears to bind more strongly to the channel, as surmised from the values for K_s. The model we have used for the cGMP-gated channel has more free parameters than can be uniquely determined in our measurements (Appendix). In fitting data, we first defined the value of the energy well (G_2) since this parameter was particularly important in defining the overall shape of the *I-V* function. We then adjusted the values of G_{12} and G_{23}. Our success in fitting the experimental *I-V* curves with one set

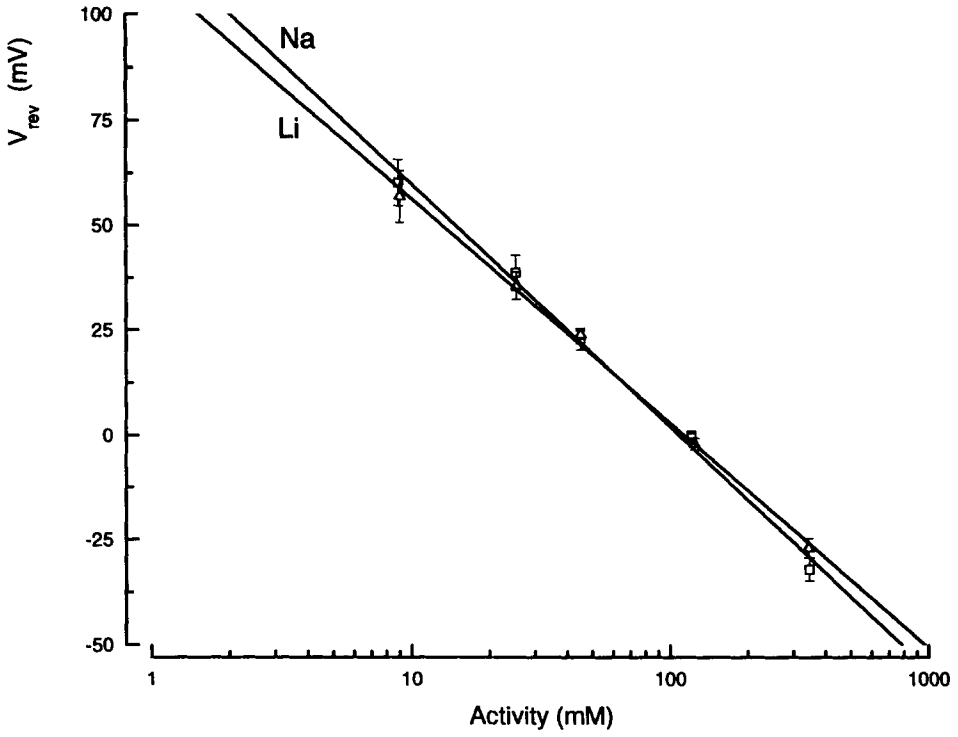

FIGURE 10. Ion selectivity of cGMP-gated channels. Reversal potentials were measured in the presence of 200 μM cGMP and ion concentration gradients. The external membrane surface was bathed with 157 mM NaCl, while the cytoplasmic surface concentration was bathed in either NaCl (*squares*) or LiCl (*triangles*) at concentrations ranging between 10 and 500 mM. In the graph, ion concentration is expressed in units of activity. The data points are the average of measurements in 14 patches for NaCl and in 6 patches for LiCl. The continuous line is the best fit to the data of the Nernst equation. The slope of the best fit line was 57.9 mV/decade activity (±3.1 SD) for Na and 53.2 mV/decade activity (±2.3 SD) for Li.

of parameters does not preclude the possibility that some other combination might also have been successful. However, once the value of only one energy barrier was defined, the choice of acceptable values for the other two was remarkably narrow.

DISCUSSION

The permeability sequence of the cGMP-gated channels of cone outer segments in bass retina is K > Na = Li = Rb > Cs. The sequence, measured in detached

membrane patches under bi-ionic conditions, is identical in single and twin cones. In a previous study in intact single cones of the tiger salamander, Perry and McNaughton (1991) reported a different sequence: Li > Na > K > Rb > Cs. This sequence, however, was inferred from measurements of the amplitude of the dark-current after rapid exchange of bathing solutions in the absence of voltage clamp. While studies in detached membrane patches are technically more reliable, since membrane voltage and the ionic composition on both sides of the membrane are under experimental control, the differences between our results and those of Perry and McNaughton probably should not be simply ascribed to details of technique or species differences. In the intact cell, unlike the detached patches studied here, fluxes of monovalent cations were measured in the presence of a large Ca concentration gradient. Since Ca ions modify the form of the *I-V* curve of the cGMP-gated channels, they may also affect their selectivity, although in intact rod photoreceptors Yau and Nakatani (1984) observed the same cation selectivity for the outer segment currents in either 1 mM or 1 μM external Ca. Investigation of the ionic selectivity in detached cone membrane patches under Ca gradients is needed to resolve the apparent differences.

In the cone outer segment membrane, current amplitude increases steeply with changes in cGMP concentration. This dependence is well described by a function (Eq. 2) which suggests that activation of the cone channels depends on the cooperative interaction of at least three cGMP molecules with a binding site in the channel of average K_m 42 μM. The value of this binding constant is weakly dependent on voltage. Haynes and Yau (1985) reported an average K_m value of 55 μM in catfish cones. cGMP-dependent currents in rod outer segment membranes are also described well by the same function, but with a different K_m (Fesenko, Kolesnikov, and Lyubarsky, 1985). Reported values for the K_m of cGMP in rods are in the range of 5 to 30 μM (reviewed in McNaughton, 1990). The K_m in rods is also weakly dependent on voltage (Karpen et al., 1988). Based on the known structure of the rod channel, and assuming that rod and cone channels are structurally analogous, these findings suggest that conductive pores in both cell types are formed by the cooperative assembly of at least three protein subunits, each of which binds a single cGMP molecule. However, the access of cGMP to the binding site differs in cone and rod channels.

The cone channels select monovalent cations over anions ideally, but exhibit only a limited ability to select among cations. The permeability sequence of the channels is similar to Eisenman's sequence IX (Eisenman and Horn, 1983). The sequences are consistent with a model of ion selectivity that presumes the presence within the conductive pore of a strong field strength cationic binding site. A similar conclusion was reached by Menini (1990) and by Furman and Tanaka (1990) for the structure of the cGMP-gated channels in rods. The selectivity gate in the channels is relatively large since arginine cations (crystal radius = 5.3 Å) permeate through the channel, yet physical dimensions alone are poor predictors of permeability since a somewhat smaller organic cation, TMA (crystal radius = 2.6 Å), does not permeate at all.

Ion channels can be recognized to be members of gene families by their common structure, generally inferred from the nucleotide sequence of their respective DNA coding molecules (Kaupp, 1991). The structure of cone cGMP-gated channels is presently unknown, but the functional similarity between cGMP-gated channels in

rod and cone photoreceptors is a strong indication that they must be members of the same gene family. Table I compares a number of functional features that have been measured in both rod and cone outer segment channels. It is clear that the channels are similar but not identical. In Fig. 11 we compare in particular detail the monovalent cation permeability and conductance sequences of cone and rod channels. Data for the selectivity of rod channels in detached membrane patches have been published by Furman and Tanaka (1990) for channels from the frog retina, and by Menini (1990) for channels from the tiger salamander retina. The data in rods in the two reports are generally similar, but our data should be more directly comparable to those of Furman and Tanaka (1990) because the conditions of their experiments are essentially identical to ours. In particular, in our solutions divalent cations were removed by 1 mM each of EGTA and EDTA. Menini used a lower concentration of divalent ion chelators and some discrepancies between her results

TABLE I

Properties of cGMP Channels in Rod and Cone Photoreceptors

	Cone	Rod
Single channel conductance		
Largest open state, *pS*	50[a], 14[b]	24[c], 25[d], 26[e], 13[b], 30[f]
cGMP binding		
K_m, μM	55[g], 42[h]	30[i], 9.6[c], 32[e], 20[f]
n	2.4[g], 2.5[h]	1.8[i], 3[c], 3[e], 3.2[f]
I-V curve with Ca present		
γ in Eq. 3	0.35[g], 0.47[h], 0.46[j]	0[k], 0[l]
Cytoplasmic cation binding constant		
Na, *mM*	104[h]	249[m]
Li, *mM*	37[h]	160[m]
Pharmacological blocker		
K_d for *l-cis*-diltiazem, μM	16[n]	3[n]

[a]Haynes and Yau, 1990; [b]Watanabe and Murakami, 1991; [c]Zimmerman and Baylor, 1986; [d]Haynes, Kay, and Yau, 1986; [e]Matthews and Watanabe, 1988; [f]Ildefonse and Bennett, 1991; [g]Haynes and Yau, 1985; [h]this report; [i]Fesenko et al., 1985; [j]Miller, J. L., and J. I. Korenbrot, manuscript submitted for publication; [k]Bader, MacLeish, and Schwartz, 1979; [l]Baylor and Nunn, 1986; [m]Menini, 1990; [n]Haynes, 1991.

and those of Furman and Tanaka might reflect incomplete chelation of divalent cations.

The *I-V* relationship of cGMP-gated macroscopic and single channel currents in cone membrane patches in the absence of divalent cations is linear between −100 and +100 mV (Haynes and Yau, 1990). In rods, in contrast, this relationship both for macroscopic (Karpen et al., 1988) and single ion currents (Ildefonse and Bennett, 1991) exhibits small outward rectification. In the presence of divalent cations the differences between rod and cone *I-V* curves persist: while the same general equation describes both curves (Eq. 3), the value of γ in Eq. 3 is not the same for rod and cone channels under comparable experimental conditions (Table I).

The interaction of monovalent cations with the cGMP-gated channels is strikingly different in rods and cones. Channels in both receptor types fail to obey the

independence principle and in both channels current amplitude reaches a saturating value as permeant cation concentration is increased (Menini, 1990). However, the binding constant for a given cation is different in rods and cones. For Na at +80 mV the K_s in cones was 104, whereas in rods at +90 mV it was 249 mM (Menini, 1990). For Li it was 37.6 in cones and 160 mM in rods (Menini, 1990; Table 1). The effect of voltage on K_s at these large depolarizing voltages is very weak, K_s decreases by ~12% for every 10 mV depolarization; thus, the quantitative difference between rod and cone channels is substantial.

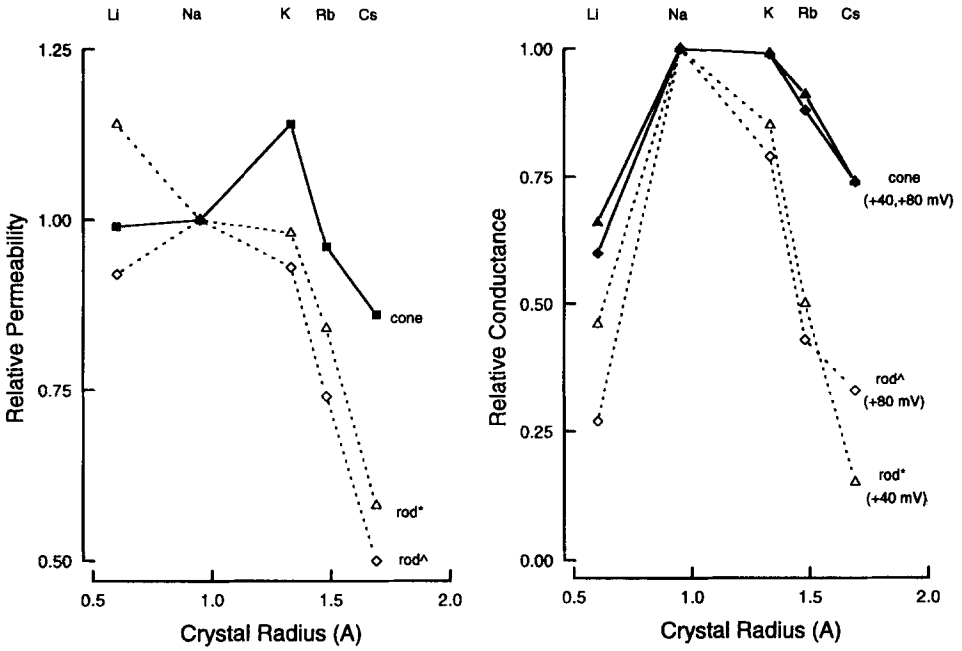

FIGURE 11. Comparison of the relative ion permeability and ion conductance in cGMP-gated channel of cones (*filled symbols*) and rods. Data for rod channels were taken from reports by Menini (1990) for tiger salamander rods (rod*, *open triangles*) and by Furman and Tanaka (1990) for frog rods (rod^, *open diamonds*). In the measurements of conductance, Furman and Tanaka (1990) reported results at +80 mV, while the values we took from Menini (1990) were those at +40 mV. We present our data at both voltages.

Eyring rate theory, as applied to membrane ion permeabilities by Zwolinski, Eyring, and Reese (1949) and Hille (1975*a*, *b*), provides a plausible model of ion channels that explains amplitude saturation and the competition observed when permeant cations are present simultaneously. This theory also explains why permeability and conductance selectivity sequences may not be the same, as we have observed. We applied this theory to an analysis of the *I-V* relationship of the cGMP-gated currents in cones measured under ion concentration gradients. The success of the theory in matching experimental data suggests that the cone outer segment channels consist of a single ion binding site separated by a single barrier from each membrane surface and that these barriers are asymmetrically located

within the membrane thickness. The binding site is occupied by one ion at a time. The difference in ion binding constants for Na and Li reflects both the difference in the depth of the energy well within the membrane and the location of the energy barriers. The difference in cation K_s between channels in rods and cones (Table I), then, reveals that the depth of the energy well is less in rods than in cones. This model of the ion channel must be regarded as an empirical description and it must be recognized that the absolute values of the physical variables invoked in the model are not exact. Nonetheless, the model provides insight into the features of the interaction of ions with the channel protein and allows us to recognize a profound difference between rod and cone cGMP-gated channels.

We have recently suggested that rods and cones differ strikingly in the kinetics of light- and voltage-dependent changes in cytoplasmic Ca concentration and, further, that this variance may be important in explaining the contrasting features of the phototransduction signals between receptor types.[1] The difference in Ca concentration kinetics, we believe, may reflect the fact that under physiological gradients the fraction of the cGMP-dependent current carried by Ca is larger in cones than in rods. Indirect measurements of Perry and McNaughton (1991) have recently suggested that this is indeed the case. Our results in this report reveal that the interaction of monovalent cation with the cGMP-gated channel is certainly different in rods than in cones. As a corollary of this finding, given the expected difference in Ca fluxes, we speculate that the interaction with Ca is less favored over that with Na in the ion binding site of the channels in cones than those in rods.

APPENDIX

The description of the *I-V* function of the cGMP-gated currents in cone outer segment membranes is based on a model that assumes that there exists within the membrane a single ion binding site located at a defined electrical distance from the membrane surfaces. This site is occupied by one ion at a time. This model was developed in detail by Hille (1975*a*, *b*) and in a general form by Lauger (1973) based on the original application by Zwolinski et al. (1949) of Eyring rate theory to the problem of membrane ionic permeability. In this model, the ion binding site is an energy well separated by two energy barriers from the cytoplasmic and extracellular membrane surfaces, respectively (Fig. 12). In the absence of an applied voltage, ions cross the energy barriers in either direction with rate constants b_{12}, b_{21}, b_{23}, and b_{32}. These rates are given by:

$$b_{12} = \frac{kT}{h} \exp\left(\frac{-(G_{12} - G_1)}{RT}\right)$$

$$b_{21} = \frac{kT}{h} \exp\left(\frac{-(G_{12} - G_2)}{RT}\right)$$

$$b_{23} = \frac{kT}{h} \exp\left(\frac{-(G_{23} - G_2)}{RT}\right)$$

$$b_{32} = \frac{kT}{h} \exp\left(\frac{-(G_{23} - G_3)}{RT}\right)$$

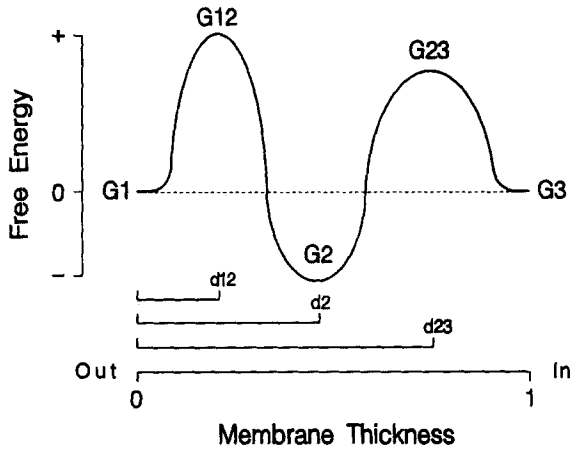

FIGURE 12. Model of cGMP-gated ion channel in cone outer segments. An ion binding site in an energy trough with free energy of activation G_2 is separated from the outside membrane surface by a barrier of free energy G_{12} and from the inside surface by a second barrier of energy G_{23}. The free energy of activation of the ions in the outside (G_1) and inside (G_3) membrane surfaces is defined as zero. Ions cross barriers G_{12} and G_{23} at rates determined by the difference in membrane voltage and in free energies across the barriers. The peaks and troughs of the energy barriers are located at electrical distances d_1, d_2, and d_3 from the outside membrane surface. These distances are in units of fraction of membrane thickness.

where k is Boltzmann's constant, h is Planck's constant, R is the universal gas constant, and T is the absolute temperature. G is the free energy of activation under standard conditions (1 M concentration). In the presence of a voltage field, V, applied across the membrane thickness, the rates now include an electrostatic term proportional to the position of the energy barrier in the membrane thickness (Fig. 12). The rate constants involving reactions with ions in the compartments outside the membrane are redefined to include an ion concentration term c (Hille, 1975*b*), assigned a value of 0.1 M, which is the usual ionic concentration in our experiments.

$$k_{12} = cb_{12} \exp\left(\frac{-(1 - d_3)zVF}{RT}\right)$$

$$k_{21} = b_{21} \exp\left(\frac{(d_3 - d_2)zVF}{RT}\right)$$

$$k_{23} = b_{23} \exp\left(\frac{-(d_2 - d_1)zVF}{RT}\right)$$

$$k_{32} = cb_{32} \exp\left(\frac{(d_1)zVF}{RT}\right)$$

Following Hille (1975*a*), the current through a single open channel in the presence of Na ions at concentrations C^i_{Na} and C^o_{Na} on the inside and outside of the membrane is expressed as:

$$I(V) = \frac{\left(\frac{c^i_{Na}}{K^i_{Na}}\right) I^i_{max} - \left(\frac{c^o_{Na}}{K^o_{Na}}\right) I^o_{max}}{1 + \left(\frac{c^i_{Na}}{K^i_{Na}}\right) + \left(\frac{c^o_{Na}}{K^o_{Na}}\right)}$$

where

$$I^{i}_{max} = zFk_{21} \quad \text{and} \quad K^{i}_{Na} = \frac{k_{21} + k_{23}}{k_{32}}$$

$$I^{o}_{max} = zFk_{23} \quad \text{and} \quad K^{o}_{Na} = \frac{k_{21} + k_{23}}{k_{12}}$$

These equations have the same form as is used in enzyme kinetics and relate the inward or outward maximum ion currents (I^{i}_{max}, I^{o}_{max}) and the ion binding constants (K^{i}_{Na}, K^{o}_{Na}) to the observed current. Equations of the same form can be used to describe bi-ionic conditions or measurements in the presence of ion mixtures (Hille, 1975*a*) by selection of appropriate constants and concentration. Thus, for the Na-Li bi-ionic solutions, with ions at concentrations C^{i}_{Li} and C^{o}_{Na}, then:

$$I(V) = \frac{\left(\frac{C^{i}_{Li}}{K^{i}_{Li}}\right) I^{i}_{max} - \left(\frac{C^{o}_{Na}}{K^{o}_{Na}}\right) I^{o}_{max}}{1 + \left(\frac{C^{i}_{Li}}{K^{i}_{Li}}\right) + \left(\frac{C^{o}_{Na}}{K^{o}_{Na}}\right)}$$

where

$$I^{i}_{max} = zFk_{21} \quad \text{and} \quad K^{i}_{Li} = \frac{k_{21} + k_{23}}{k_{32}}$$

$$I^{o}_{max} = zFk_{23} \quad \text{and} \quad K^{o}_{Na} = \frac{k_{21} + k_{23}}{k_{12}}$$

To describe the amplitude of macroscopic currents, single open channel currents calculated with the equations above must be multiplied by the number of channels being sampled and their probability of opening. Because neither of these two parameters are known for the channels we study here, in our application of this theory we selected an arbitrary scaling coefficient by matching the amplitude of the simulated and experimental current amplitudes at +80 mV.

We thank J. Miller, D. Julian, and N. Dwyer for their valuable comments on this manuscript. We thank A. Zimmerman and D. Baylor for communication before publication of their study on ion permeabilities in rod cGMP-gated channels.

Research was supported by grant EY-05498 from the National Eye Institute.

Original version received 11 February 1992 and accepted version received 28 April 1992.

REFERENCES

Attwell, D., F. S. Werblin, and M. Wilson. 1982. The properties of single cones isolated from the tiger salamander retina. *Journal of Physiology.* 328:259–283.

Bader, C. A., P. R. MacLeish, and E. A. Schwartz. 1979. A voltage-clamp study of the light response in solitary rods of the tiger salamander. *Journal of Physiology.* 296:1–26.

Baylor, D. A., and B. J. Nunn. 1986. Electrical properties of the light-sensitive conductance of rods of the salamande Ambystoma tigrinum. *Journal of Physiology.* 371:115–145.

Cherr, G. N., and N. L. Cross. 1987. Immobilization of mammalian eggs on solid substrates by lectins for electron microscopy. *Journal of Microscopy.* 145:341–345.

Eisenman, G., and R. Horn. 1983. Ion selectivity revisited: the role of kinetic and equilibrium processes in ion permeation through channels. *Journal of Membrane Biology.* 76:197–225.

Eyring, H., R. Lumry, and J. W. Woodbury. 1949. Some applications of modern rate theory to physiological systems. *Records of Chemical Progress.* 10:100–114.

Fesenko, E. E., S. S. Kolesnikov, and A. L. Lyubarsky. 1985. Induction by cyclic GMP of cationic conductance in plasma membrane of retinal rod outer segments. *Nature.* 313:310–313.

Furman, R. E., and J. C. Tanaka. 1990. Monovalent selectivity of the cyclic guanosine monophosphate-activated ion channel. *Journal of General Physiology.* 96:57–82.

Hamill, O. P., A. Marty, E. Neher, B. Sakmann, and F. J. Sigworth. 1981. Improved patch-clamp techniques for high-resolution current recording from cells and cell-free membrane patches. *Pflüger Archiv.* 391:85–100.

Haynes, L. W. 1991. Block of the cGMP-gated channel of rod and cone photoreceptors by l-cis-diltiazem. *Biophysical Journal.* 59:539*a*. (Abstr.)

Haynes, L. W., A. R. Kay, and K.-W. Yau. 1986. Single cyclic GMP-activated channel activity in excised patches of rod outer segment membranes. *Nature.* 321:66–70.

Haynes, L. W., and K.-W. Yau. 1985. Cyclic GMP-sensitive conductance in outer segment membrane of catfish cones. *Nature.* 317:61–64.

Haynes, L. W., and K.-W. Yau. 1990. Single-channel measurements from the cGMP-activated conductance of catfish retinal cones. *Journal of Physiology.* 429:451–481.

Hestrin, S., and J. I. Korenbrot. 1987. Effects of cyclic GMP on the kinetics of the photocurrent in rods and in detached rod outer segments. *Journal of General Physiology.* 90:527–551.

Hille, B. 1975*a*. Ionic selectivity of Na and K channels of nerve terminals. *In* Membranes: A Series of Advances. Vol. 3. G. Eisenman, editor. Marcel Dekker Inc., New York. 255–323.

Hille, B. 1975*b*. Ionic selectivity, saturation and block in sodium channels. *Journal of General Physiology.* 66:535–560.

Hille, B. 1984. Ionic Channels of Excitable Membranes. Sinauer Associates, Inc., Sunderland, MA. 426 pp.

Hodgkin, A. L., and B. Katz. 1949. The effect of sodium ions on the electrical activity of the giant axon of the squid. *Journal of Physiology.* 108:37–77.

Hodgkin, A. L., P. A. McNaughton, and B. J. Nunn. 1985. The ionic selectivity and calcium dependence of the light-sensitive pathway in toad rods. *Journal of Physiology.* 358:447–468.

Ildefonse, M., and N. Bennett. 1991. Single-channel study of the cGMP-dependent conductance of retinal rods from incorporation of native vesicles into planar lipid bilayers. *Journal of Membrane Biology.* 123:133–147.

Karpen, J. W., A. L. Zimmerman, L. Stryer, and D. A. Baylor. 1988. Molecular mechanics of the cyclic GMP-activated channel of retinal rods. *Cold Spring Harbor Symposia on Quantitative Biology.* 53:325–332.

Kaupp, U. B. 1991. The cyclic nucleotide-gated channels of vertebrate photoreceptors and olfactory epithelium. *Trends in Neuroscience.* 14:150–157.

Korenbrot, J. I., and A. V. Maricq. 1991. Calcium channels in sensory transduction: a case study in photoreceptors. *In* Calcium Channels: Their Properties, Functions, Regulation and Clinical Relevance. L. Hurwitz, L. D. Partridge, and J. K. Leach, editors. CRC Press, Inc., Boca Raton, FL. 107–123.

Lauger, P. 1973. Ion transport through pores: a rate-theory analysis. *Biochimica et Biophysica Acta.* 311:423–441.

Matthews, G., and S.-I. Watanabe. 1988. Activation of single ion channels from toad retinal rod inner segment by cyclic GMP: concentration dependence. *Journal of Physiology.* 403:389–405.

McNaughton, P. A. 1990. Light response of vertebrate photoreceptors. *Physiological Reviews.* 70:847–883.

Menini, A. 1990. Currents carried by monovalent cations through cyclic GMP-activated channels in excised patches from salamander rods. *Journal of Physiology.* 424:167–185.

Menini, A., G. Rispoli, and V. Torre. 1988. The ionic selectivity of the light-sensitive current in isolated rods of the tiger salamander. *Journal of Physiology.* 402:279–300.

Perry, R. J., and P. A. McNaughton. 1991. Response properties of cones from the retina of the tiger salamander. *Journal of Physiology.* 433:561–587.

Pugh, E. N., Jr., and W. H. Cobbs. 1986. Visual transduction in vertebrate rods and cones: a tale of two transmitters, calcium and cyclic GMP. *Vision Research.* 26:1613–1643.

Pugh, E. N., Jr., and T. D. Lamb. 1990. Cyclic GMP and calcium: the internal messengers of excitation and adaptation in vertebrate photoreceptors. *Vision Research.* 30:1923–1948.

Robinson, R. A., and R. H. Stokes. 1965. Electrolyte Solutions. Butterworth and Co., Ltd., London. 571 pp.

Watanabe, S.-I., and M. Murakami. 1991. Similar properties of cGMP-activated channels between cones and rods in the carp retina. *Visual Neuroscience.* 6:563–568.

Yau, K. W., and D. A. Baylor. 1989. Cyclic GMP-activated conductance of retinal photoreceptor cells. *Annual Review of Neuroscience.* 12:289–327.

Yau, K. W., P. A. McNaughton, and A. L. Hodgkin. 1981. Effects of ions on the light-sensitive current in retinal rods. *Nature.* 292:502–505.

Yau, K. W., and K. Nakatani. 1984. Cation selectivity of light-sensitive conductance in retinal rods. *Nature.* 309:352–354.

Zimmerman, A. L., and D. A. Baylor. 1986. Cyclic GMP-sensitive conductance of retinal rods consists of aquaeous pores. *Nature.* 321:70–72.

Zimmerman, A. L., J. W. Karpen, and D. A. Baylor. 1988. Hindered diffusion in excised patches from retinal rod outer segments. *Biophysical Journal.* 54:351–355.

Zwolinski, B. J., H. Eyring, and C. E. Reese. 1949. Diffusion and membrane permeability. *Journal of Physical Colloidal Chemistry.* 53:1426–1453.